Measuring and Observing Diffraction Patterns and Determining Geometries by Razorblade and Pinhole Profiling and Microscope Measurement

Benjamin Schreyer

April 29th 2023

1. Abstract

The diffraction pattern of various machined diffraction slits were measured with two methods, one by simply imaging light intensities at different points along an axis of space, the pinhole method. The other by using a blocking razor blade and collecting lens to measure an integrated intensity of the beam, the razorblade method. Airy Diffraction was also observed by eye, however no quantitative data was taken. The results of these measurements were compared with theory, and used to calculate values for the geometry of the diffraction slits. The two methods of profiling are also compared, and a third measurement of the slits was conducted using a microscope with distance crosshair. Diffraction slits of counts $1,2,3,4,5$ were measured. Razorblade profiling of diffraction profiles proved to be much faster than pinhole profiling due to smaller pattern size. The microscope measurement of slit geometry, the diffraction measurement of slit geometry, and the manufacturer listed slit geometries generally agreed, although some values were affected by significant systematic error. Below are listed values measured for the geometry of the slits, with underlined values being identified as seriously affected by systematic error. Refining this experiment would have the first steps of more careful use of a microscope when measuring slit geometry.

Airy Rings Airy Diffraction was not analyzed numerically here and so theoretical results are not needed, besides that the Airy diffraction pattern should appear radially symmetric, and have oscillating intensity with the radial coordinate, with oscillation amplitude going to zero for large radii on the target/observation plane. These are the qualities expected of an airy ring that one could expect to observe with the naked eye.

Diffraction Profiling Slit Geometry Values Fit Parameters for Slit Width, Separation. Note, convergence was failing for some of these fits in the submitted lab notebook. Changing initial guess parameters, and including the aperture in the theoretical model, let the curve fitting routine converge much more nicely, which is reflected in this report.

Aperture Width The apparent aperture width along the pattern was found to be $0.002m \pm 0.0001m$ for pinhole imaging. The error bars were found by applying brute force grid search on the integer parameter for the width of the discrete convolution filter modeling the aperture. The two nearest neighbors are considered viable to be conservative. One is conservative here incase the possible integer spaced values for width $\Delta = 0.1mm$ are not fine enough to well distinguish two different slit widths that are realizable with the physical aperture.

Table 1

Method	Num. Slits	Slit Width, Error:(Upper, Lower)mm	Slit Seperation (Upper, Lower)mm
Pinh.	1	0.080 (0.076, 0.084)	NA
Pinh.	2	0.043 (0.041, 0.045)	0.127 (0.121, 0.132)
Pinh.	3	0.044 (0.042, 0.046)	0.127 (0.121, 0.132)
Pinh.	4	0.044 (0.042, 0.046)	0.126 (0.121, 0.132)
Pinh.	5	0.044 (0.042, 0.046)	0.126 (0.121, 0.132)
Razor	1	0.090 (0.067, 0.112)	NA

Microscope Slit Geometry Values Microscope Measurements For Slit Width, Separation. Microscope was out of focus for measurement of underlined values, and thus these values may be inflated significantly above their true value.

Table 2

Num. Slits	Slit Width mm	Slit Separation mm
1	0.083 ± 0.004	NA
2	$\underline{0.051} \pm 0.004$	$\underline{0.130} \pm 0.004$
3	$\underline{0.051} \pm 0.004$	$\underline{0.130} \pm 0.004$
4	$\underline{0.051} \pm 0.004$	$\underline{0.130} \pm 0.004$
5	$\underline{0.051} \pm 0.004$	$\underline{0.130} \pm 0.004$

Manufacturer Slit Geometry Values Manufacturer did not provide error bars.

Table 3

Num. Slits	Slit Width mm	Slit Separation mm
1	0.08	NA
2	0.04	0.125
3	0.04	0.125
4	0.04	0.125
5	0.04	0.125

2. Introduction

This experiment measured geometry of small slits by two methods, microscope viewer with distance crosshair, and fitting of a theoretical model to a diffraction pattern created by the slits when red ($635nm \pm 1nm$) laser light was incident upon them perpendicularly. Within ways to obtain diffraction patters created by these slit geometries, two were used, razorbalde blocking, and pinhole sweep. The pinhole method is more simplistic to understand, and provides simpler to interpret data, however proves to be slower. The microscope viewer as a tool is relatively straight forward in its operational properties, however dealing with it as a physical system does prove to be time consuming and is significantly sensitive to misconfiguration. These methods are described further.

2.1. Diffraction Patterns

Diffraction occurs when coherent light passes through a geometrical aperture or object. These patterns can be seen with the eye, and measured as described further. The theoretical result for Fraunhofer diffraction through one or more rectangular slits is as follows, extended to include the contrast c and asymmetry ϕ due to imperfections in the lab setup. In addition as a final correction for finite pinhole aperture, a convolution with an averaging filter is added, which models the width of the physical aperture, and its equal receptivity to photons over its entire width.

$$I = I_0(\frac{sin\beta}{\beta})^2((1-c)+c\frac{sinN(\alpha-\phi)}{sin(\alpha-\phi)})^2 \tag{1}$$

$$\beta = \frac{\pi}{\lambda}b\frac{y}{L} \tag{2}$$

$$\alpha = \frac{\pi}{\lambda}a\frac{y}{L} \tag{3}$$

$$I_{model/final} = I \star a(x) \tag{4}$$

Here $a(x)$ is the aperture defined as $a(x) = 1; |x| < 0.5 \cdot w_a,\ 0\ ; otherwise.$ Constant w_a is the width of the aperture. $\star$ denotes convolution, which is a mathematically simple way to express the rolling average.

Coherent light is incident on small slits and emits with spherical wave fronts from these slits, until it is incident on a surface sufficiently far away (discussed later).Where y is the displacement along the axis which the pattern appears, L is the distance from the slits to the target, λ is the wavelength of the light. I_0 is the intensity of the light incident on the slits. N is the number of slits.Variables a, b are the distance each slit is from the next, and the width of the slits respectively. We want to measure these intensity profiles with real slits. These equations are only valid for $L \gg \frac{b^2}{2\lambda}$. Parameter c corrects for deviations in slit geometry and beam intensity. It however cannot correct for aliasing as described in methods. ϕ corrects for rotation of the slits causing asymmetric curves about their center. Finally to this theoretical model, when using the pinhole method, with a large aperture as required by physical limitations of the experimental apparatus, our model gets an added convolution applied averaging filter, which models well an aperture of finite size. The apparent aperture width along the pattern was found to be $0.002m \pm 0.0001m$ for pinhole imaging, which is about the feature width of the diffraction pattern. Given the size of our pinhole we expect to be able to discern the first order peaks, as will be made more mathematically evident further.

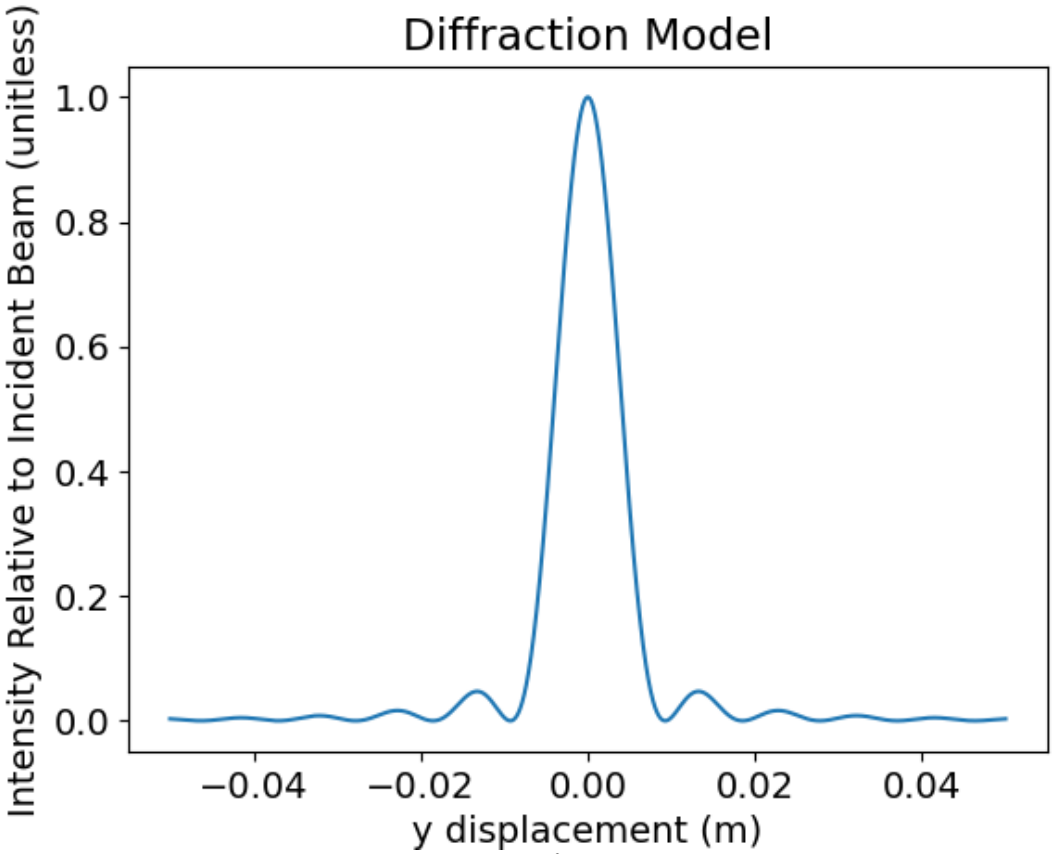

Figure 1: Example plot for the theoretical model, $\lambda = 650nm$, $N = 1$, $b = 0.08mm$, $L = 1m, \phi = 0, c = 1$

2.2. Pinhole Method for Measuring Diffraction Patterns

A photodiode and aperture (the ”pinhole” we use) are used to measure beam intensity in the pinhole method, since we assume that the manufacturer has provided a diode who’s voltage is proportional to incident photon intensity up to saturation, and including noise. We take the correlation between photodiode voltage and light intensity as given, with regard for saturation, noise, and alignment failure. The pinhole also is not infinitely small, and thus does not ideally image the beam, this is discussed in methods. The pinhole measures an integrated intensity over the aperture size of the pinhole, which as the pinhole shrinks approaches the true intensity at the point. The pinhole method can be used to profile a diffraction pattern. The diffraction pattern’s y axis is the axis for which the beam is profiled along, as it provides information about the slit separations and widths by its pattern of diffraction.

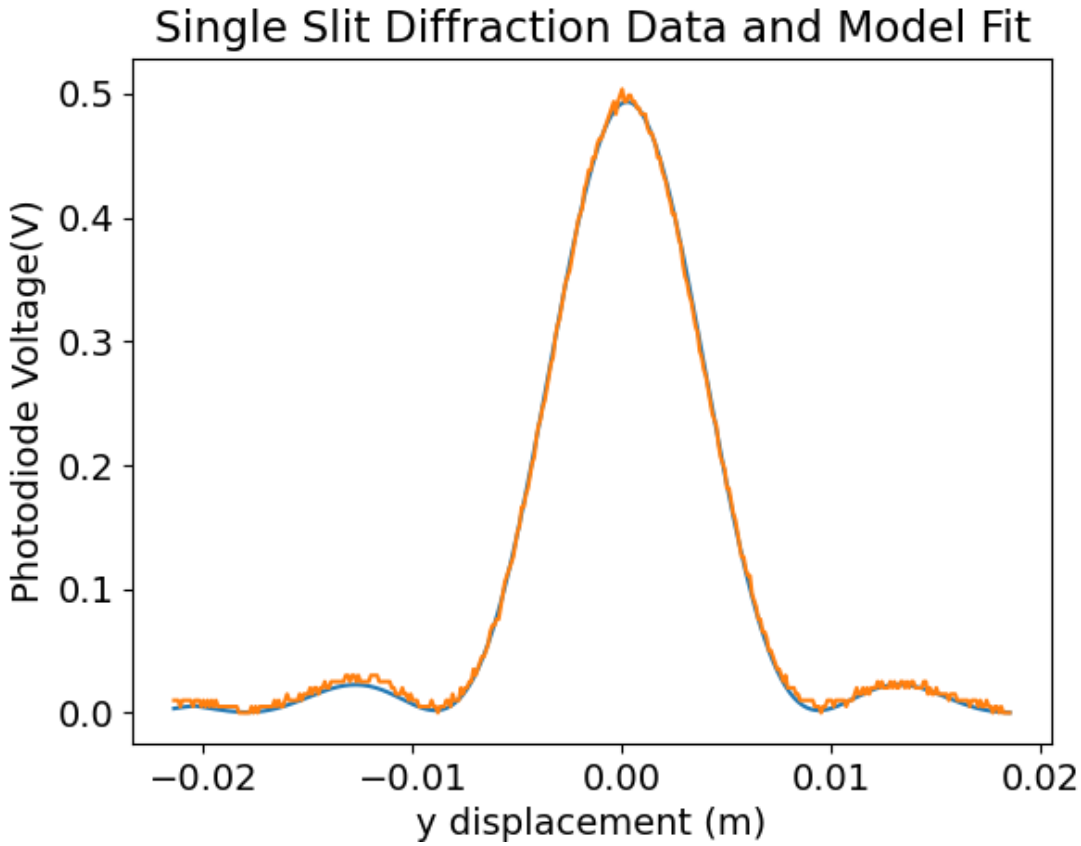

Figure 2: Pinhole method data plotted. Included also, a plot of the theoretical model with fitted parameters.

2.3. Razorblade Method for Measuring Diffraction Patterns

The razorblade method measures the integrated diffraction profile by blocking part of the diffraction pattern and then using a lens to collect the unblocked pattern onto a photodiode. summing all photon intensities, giving an integrated beam intensity, for each displacement of the blocking aperture. A fully blocked measurement would have no laser light incident onto the collecting lens, the fully unblocked case would ideally have all of the patterns light incident on the lens, since none is incident on the blocking target. Inbetween lie integrals of the pattern intensity with varying bounds. The razorblade method provides the same information as the pinhole method, the diffraction pattern, however it provides an integrated form of the pattern. Taking a finite derivative to recover the nonintegrated pattern increases noise significantly. To avoid such noise and invert the integration of the pattern, a linear transformation composed of a rolling average filter, and the finite difference is used to calculate the spatial distribution of pattern intensity.

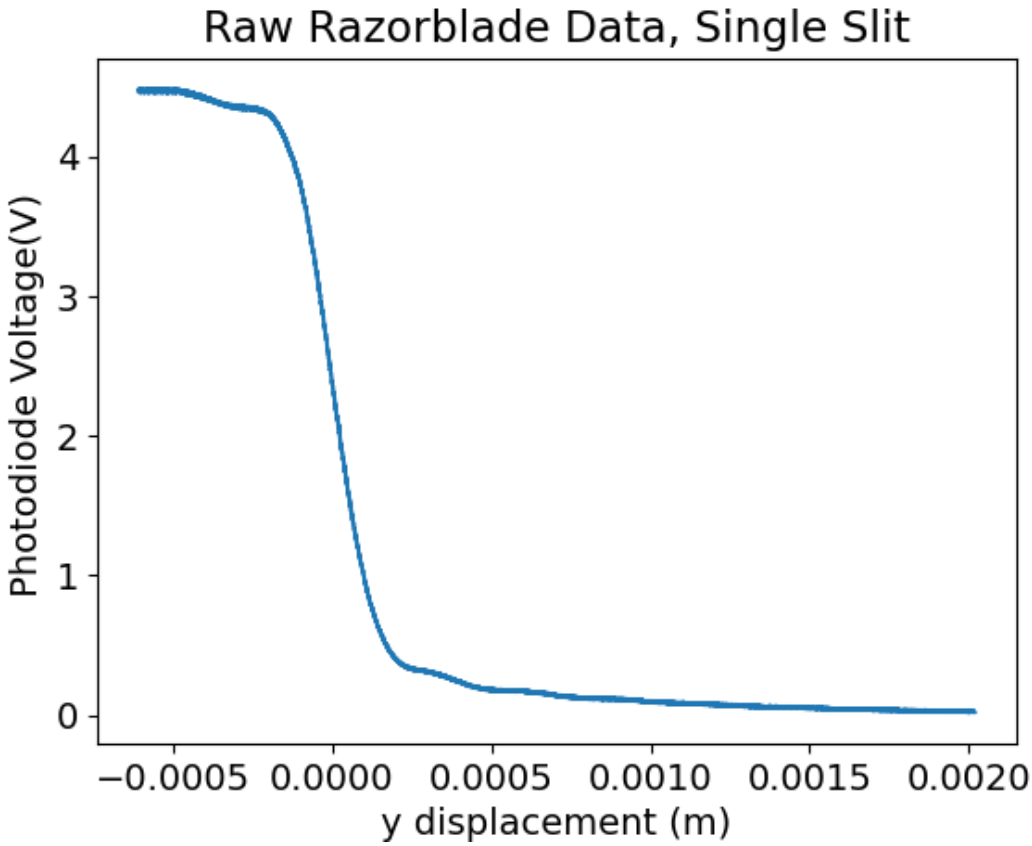

Figure 3: Raw data read in from razorblade profiling of a single slit diffraction.

2.4. Fitting Diffraction Patterns to Theory to Extract Slit Geometry

By assuming the validity of the diffraction theoretical model, slit widths can be determined from measured diffraction patterns. Fit parameters are those described in the theoretical model, importantly slit width and separation(separation if more than one slit is present). We hold parameters: the number of slits, distance from slits to observation plane, and wavelength of laser light constant, since we have knowledge of these parameters, and cannot have multiple degrees of freedom for each characteristic of our diffraction pattern. Otherwise there will be multiple valid theoretical explanations for them. Both the pinhole and razorblade method produce intensity profiles that can be fit to these theoretical models, yielding slit width and separation parameters.

2.5. Microscope for Measuring Slit Geometry, Validation of Model

A microscope was used to measure slit widths and separations. This provides the second method of determining the slit width and separation, which in turn can be used to validate the diffraction model used, since the slit widths produced by the diffraction model, and the measured slit widths directly by microscope can be compared for varying numbers of slits. The number of slits was provided by the manufacturer and confirmed using the microscope.

3. Methods

Slits of various sizes, counts, and separations were available already manufactured. These slits were used to create diffraction patterns by shining $635nm \pm 1nm$ laser light directly onto the slits, and determining the pattern of light created by profiling. By either partially blocking the beam with a stepper actuated stage mounted business card and measuring how much light passed, or by directly measuring an apertured photodiode reading at various points, the pattern of light was determined over space at an observing plane $114cm \pm 5cm$ away (in the case of pinhole profiling), or $4cm \pm 1cm$ away in the case of the razorblade method.

3.1. Pinhole Pattern Measurement

To measure the pattern with a pinhole apertured photodiode, first the laser is shone onto the diffraction slits. Then at $114cm$ a motorized stage is placed with the apertured photodiode. We consider the aperture size, as to collect enough detail of the pattern, in our case about equal to the smallest width we wish to resolve in the pattern. See futher discussion in methods for how this aperture size was determined. The aperture cannot be made too small, as then no reading will be given at the photodiode, noise will dominate. Regardless of aperture size the apertured photodiode is swept across an axis perpendicular to the laser beam if it was uninterrupted by slit geometry, and perpendicular to the long axis of the slit geometries. An example of data collected is shown in 2. In this case the Fraunhofer limit is $114cm \gg \frac{0.008cm^2}{2 \cdot 635 \cdot 10^{-7} cm}$

3.2. Razorblade Pattern Measurement

To measure the diffraction of the laser light with a pattern scan that is much shorter than the pinhole method, a similar configuration is used but with a blocking target that moves along the same axis that the apertured photodiode moves instead of moving the photodiode itself. After the laser which shines perpendicularly onto the slit geometry, the motor driven stage is set $4cm \pm 1cm$ away, and holds a blocking piece of paper. The paper is moved from completely allowing the pattern to continue on, to completely blocking it. After the blocking motorized stage, a focusing lens is used to collect the laser light that was not blocked. The focus of this lens is set on the photodiode, so that is records a voltage proportional to the total light intensity collected by the lens. Example data for this method was plotted in 3. Because the razorblade method does not have a pinhole that makes alignment much more difficult, scans of the pattern can be done much closer to the photodiode, while still capturing fine enough detail of the pattern to fit parameters (Still within the Fraunhofer limit $L \gg \frac{b^2}{2\lambda}$). In this case the Fraunhofer limit is $4cm \gg \frac{0.008cm^2}{2 \cdot 635 \cdot 10^{-7} cm}$.

3.3. Pinhole Method Curve Fitting

The curves produced by pinhole pattern profiling are immediately able to be fit to the diffraction theory 1. Again the parameters c, ϕ account for further imperfections in the experimental setup that are still predictable via modeling. Constant background noise incident on the photodiode was accounted for by making the minima of the measured data zero by appropriate placewise subtraction of a constant. A curve fitting package is used, in our case Scipy with Python 3 to fit the parameters to the measured data. When provided with a typical deviation for each data point, our curve fitting package can provide error estimates for parameters due to this point error. The estimated error in parameters due to these point deviations was always at least 100 times smaller than error caused by deviation in the length measurement between the diffraction slits, and the observation plane. As a

result error due to point deviations was ignored as it was insignificant, and instead to determine error bounds, curve fits were done with different values for the distance L. $L = 114cm$ was measured, however our uncertainty in this figure was $5cm$. To determine how this affected parameter fits, L was set to have values at the upper bounds of this error $119cm, 109cm$ and then the free parameters were fit for both. All combinations of these maximal error deviations were tried, and the most extremely deviated values of a, b due to this change in set parameter L were chosen as a range for possible values of parameters a, b. This was also applied with the known/set parameter $\lambda = 635nm \pm 1nm$ which had a much smaller error, but was still included for consistency.

Aperture Width The apparent aperture width along the pattern was found to be $0.002m \pm 0.0001m$ for pinhole imaging. The error bars were found by applying brute force grid search on the integer parameter for the width of the discrete convolution filter modeling the aperture. The two nearest neighbors are considered viable to be conservative. One is conservative here incase the possible integer spaced values for width $\Delta = 0.1mm$ are not fine enough to well distinguish two different slit widths that are realizable with the physical aperture.

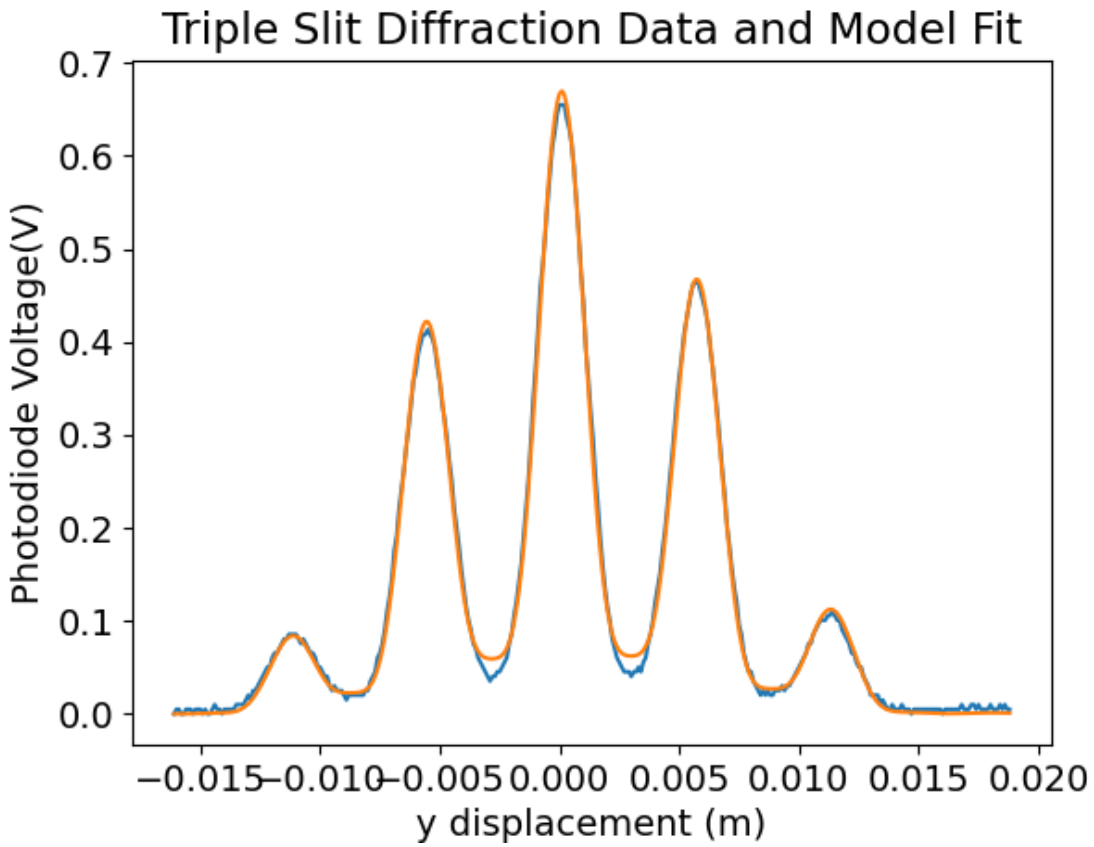

Figure 4: Example curve fit for $N = 3$ triple slits. the theoretical model expected secondary peaks between the larger peaks, but the size of the pinhole aperture, as will be discussed further, destroys this level of detail in our measured data.

As the number of slits increases and other parameters are held constant, the peaks of the pattern are predicted to become sharper by theory, however the finite size of the aperture will for enough

peaks, distort this effect. This is clear when determining a fit for four or more slits. The finite aperture model is very important for convergence of fits as one can see in 7.

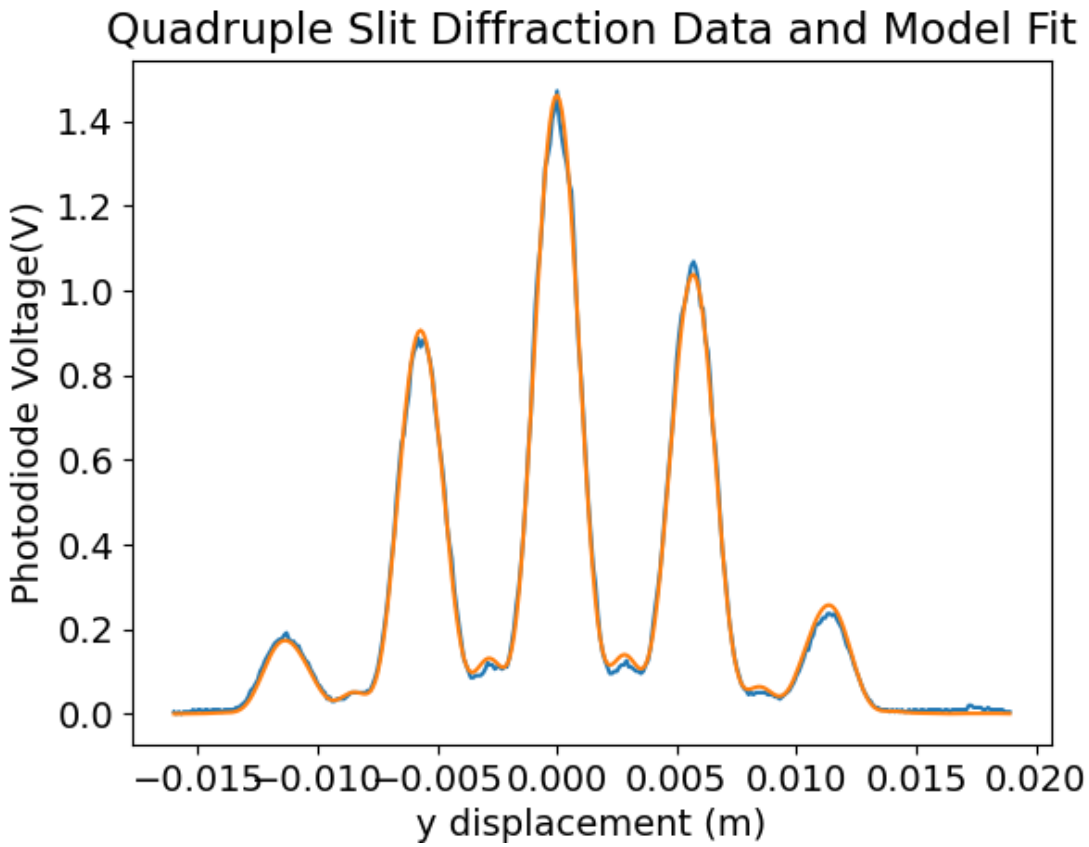

Figure 5: The measured profile, by pinhole, for the four slit diffraction grating. The large aperture size becomes very significant, flattening and widening sharper peaks and obscuring fine details.

This effect becomes even more pronounced for five slits.

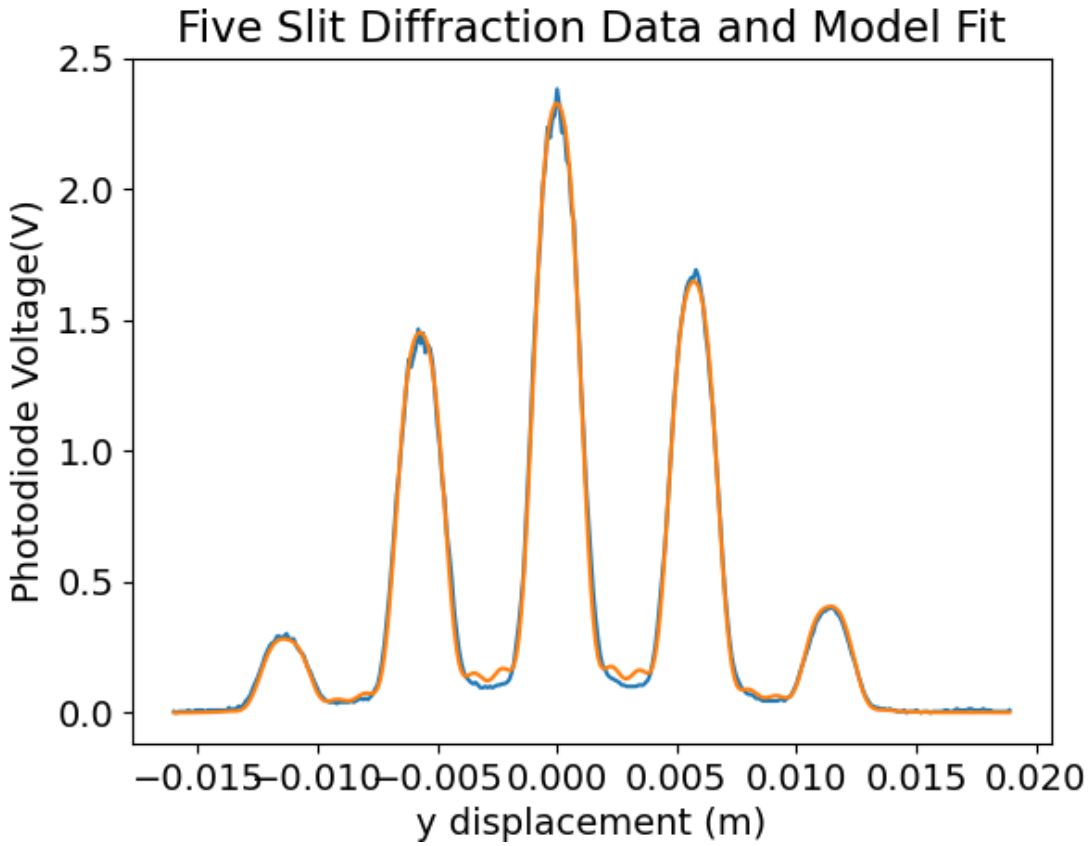

Figure 6: Five slit diffraction measured data and curve fit.

This effect becomes even more pronounced for five slits.

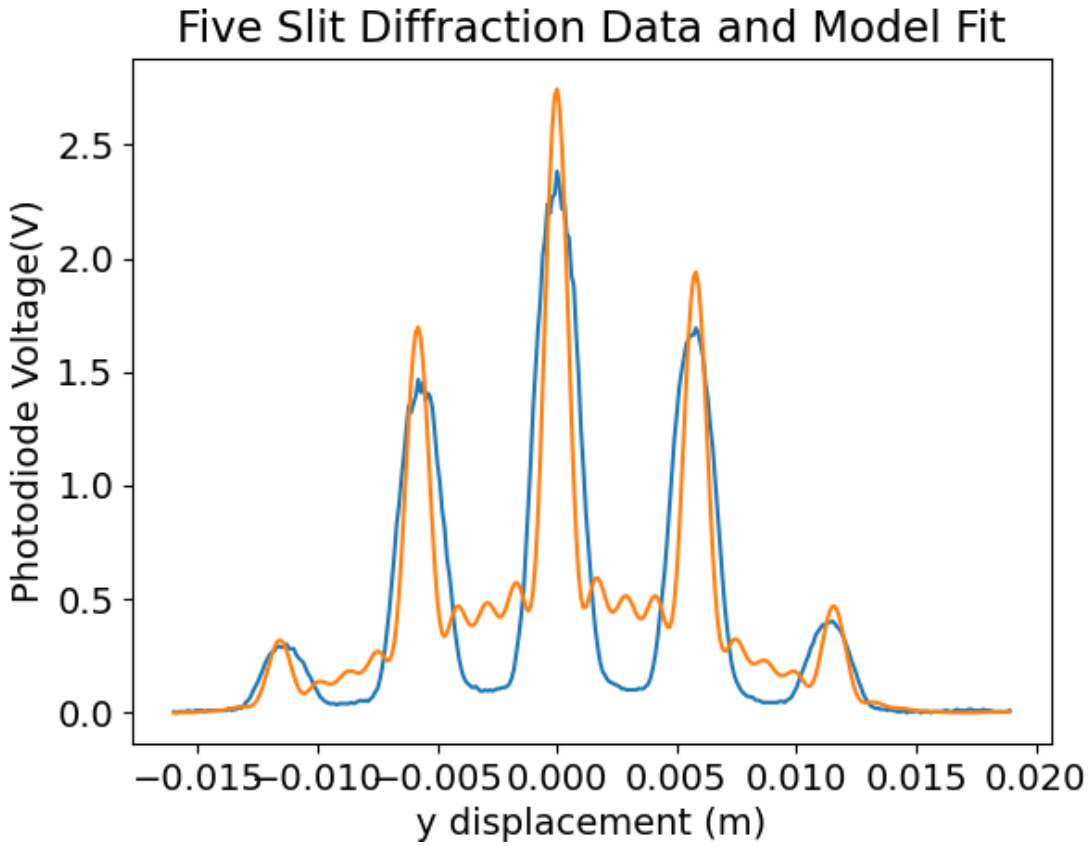

Figure 7: Five slit diffraction measured data and curve fit without finite aperture modeled by rolling average. Note that convergence is much worse, and the model is unable to accommodate the data.

3.4. Razorblade Method Curve Fitting

As discussed, the data that is collected by the razorblade method is an integrated curve of the actual diffraction pattern, resulting in the raw data 3. To recover a function that has been integrated, a derivative must be taken. In this case a finite derivative, since our data is discrete in nature.

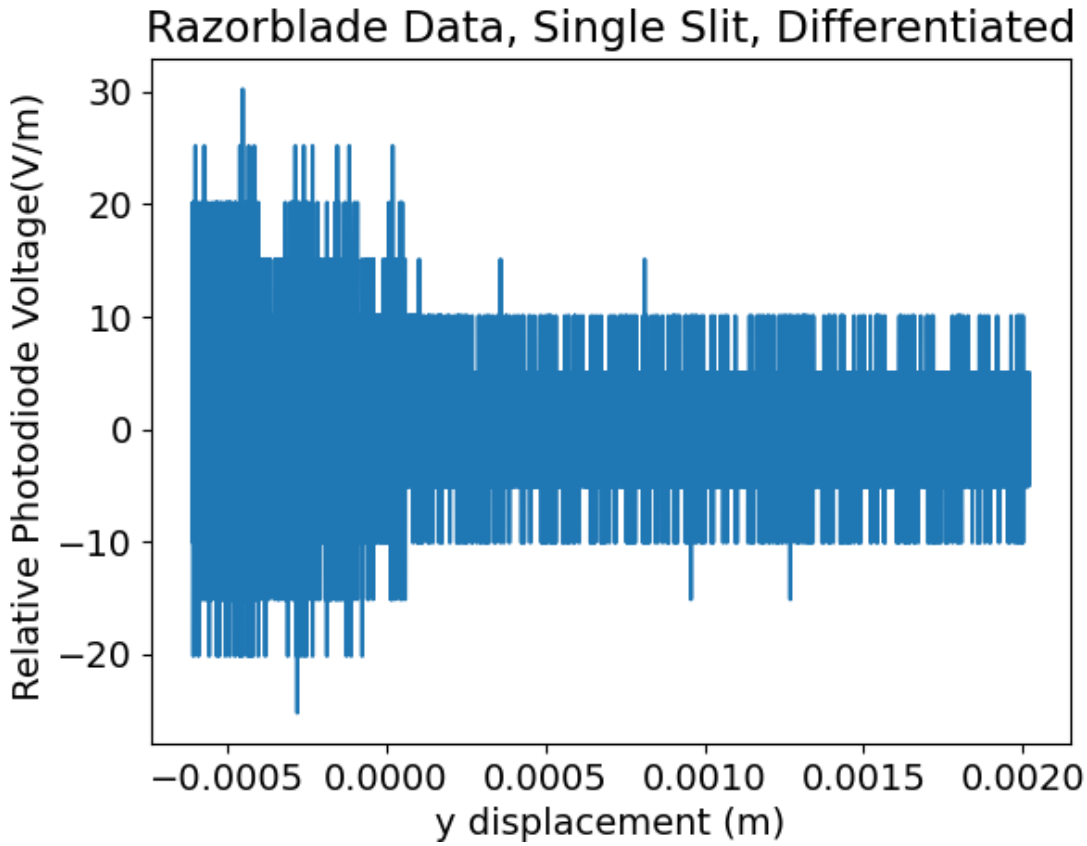

Figure 8: Differentiated razorblade data. Noise is amplified by the finite derivative, because it has a high frequency relative to the theoretical diffraction pattern. A heuristic for this is $\frac{d}{dx}e^{irx} = ire^{irx}$, note the factor of r. The bigger the frequency, the greater the amplification when derivative is applied. A more careful treatment of such ideas is given further, but this heuristic is highly analogous to the discrete case.

To allow for more intuitive plotting, and less finicky curve fitting, this noise must be removed. By applying a rolling average filter to this data, high frequency noise can be removed, it turns out we want a filter size of $n = 1000$ data point averaging. Why this is so is explained further.

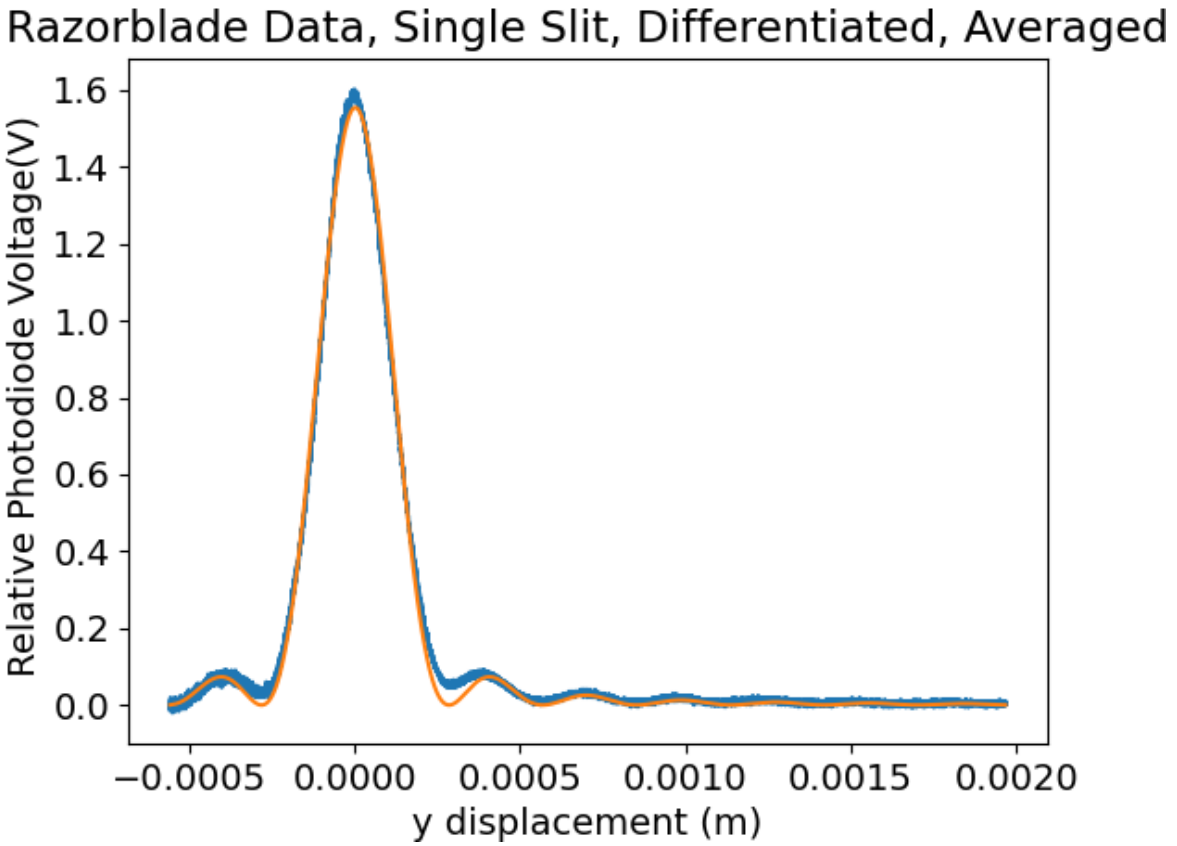

Figure 9: Raw data read in from razorblade profiling of a single slit diffraction, now with finite derivative applied and filtered by an average $n = 1000$. In orange a curve fit is given for single slit diffraction aswell. Note the units of volts now that averaging has been applied. The voltage is scaled linearly by an arbitrary amount to make the plot readable, since the parameters of slit width and separation do not vary with such linear modulation. The expected diffraction pattern is recovered.

Once the razorblade data is filtered and differentiated, the same error analysis techniques can be used as for the pinhole method, since the data at this stage is of the same form. There is increased point error due to the finite derivative, however its contribution to slit width and separation parameter error is still as before at least 100 time smaller than error due to distance measurement imperfections, and can also be ignored. Data was only taken for the single slit using the razor blade method.

3.5. Linear Filters

Linear filtering of signals is easily described with the Fourier transform or discrete Fourier transform. Both the finite derivative and rolling average filter are linear filters and can be considered through this lens.

Feature Size Dependent Damping A linear rolling filter, and the data it is applied to can be looked at in a Fourier basis, feature size, as used for our purposes, means the ”wavelength” parameterization of Fourier modes, feature frequency is the ”frequency” or k-space parameterization of Fourier modes. Such filters also introduce variable damping of different feature sizes. The diffraction curves are approximately singular in their feature sizes, if one only pays attention to the first order mode. If one wants to compare the effect of this on different modes, it is not

too complex (Linear Filtering/Convolution, analyzed in the Fourier domain is the math behind this $FT[f(x) \star f_{filter}(x)] = FT[f] \cdot FT[f_{filter}]$). It is conventient to look at rolling filters through the lens of frequency dependent gain, because different frequencies define different feature sizes $G(\omega) = FT[f_{filter}]$. For our purposes the filter is a square wave, and f is the diffraction pattern. The Fourier transform of a square wave is a sinc function, which in our application, in accordance with aliasing theory, will be close to constant when $FT[f(x)]$ has significant magnitude (which is for relatively small frequencys, which are the same as relatively large feature sizes), leaving the signal intact. For a mathematically perfect aperture absorbing all incident light (apertures act as an averaging filter, and vice versa), the factor in front of $FT[f]$ for exactly the criterion $\omega_{sampling} = 2 \cdot \omega_{feature}$ will only drop to at minimum 0.8 relative to its maximum value (which is for a constant signal). If $\omega_{sampling} = \omega_{feature}$ the value of the coefficient $FT[f_{filter}]$ drops to below 0.5. The important takeaway here is that if we size our aperture appropriately, we can deduce different sized features, and their relative magnitudes will not be biased too heavily, ie our filter will not make higher frequency but still unaliased peaks look an order of magnitude smaller than they should appear (only up to a 20% difference in an extreme case).

In Pinhole Profiling In pinhole profiling, where our feature size and filter width were approximately equal, we expect up to 25% amplitude loss for the sharpest large peaks due to the aperture. Plots 6, 7, show this well, by giving model fits with an without aperture portions of the model. The sharp theoretical peaks viewed with an infinitely small aperture are significantly higher than the the apertured peaks despite having converged to the same slit width and separation parameters (the same qualifies within less than 5%)

Relating the two profiling methods The razorblade technique provides an integrated intensity profile of the originial profile. As a result one uses the finite derivative to recover the true shape of the intensity profile from a razorblade profile. This derviative's noise will be large, because the spatial finite derivative amplifies high frequency signals, which are present when the stepper is single stepped and electronic noise is significant. This magnifies small electrical and digitization noise. Because this noise is distributed around zero, it can be removed by a simple averaging filter. By using the razorblade method we now control our aperture size during analysis, and determine the behavior of such averaging by seeing filtering through the lens of linear filters, specifically, convolution. In our case we set the filter width to be 1000 steps. This number was determined by two metrics. First the width of the peaks to be imaged is greater than 3000 steps, meaning we will not have aliasing. Secondly when looking at the depression of signal for this feature size it is at worst 98%, when applying a the 1000 step width software filter for the razorblade technique. Observe on the enveloping function for the averaging filter, that for feature sizes with frequency $\omega = \omega_{filter}\frac{1}{3}$ the signal is hardly modulated below a factor of 1.0. Since our filter is 1000 steps wide, and our feature is 3000 steps wide at its finest details (for the single slit diffraction and its theoretical model), we know that distortion of the signal by such a filter will be on of only $1-2\%$. Importantly phase shifting is not variable with feature size, besides flip of sign for the finite derivative and rolling average, so phase shift is uniform, and can be ignored, ie we can look at the response of such filters as a real valued function, with the caveat that we may need to add a complex phase at the end of calculation if it is relevant to our system, which it is not the case for diffraction pattern analysis.

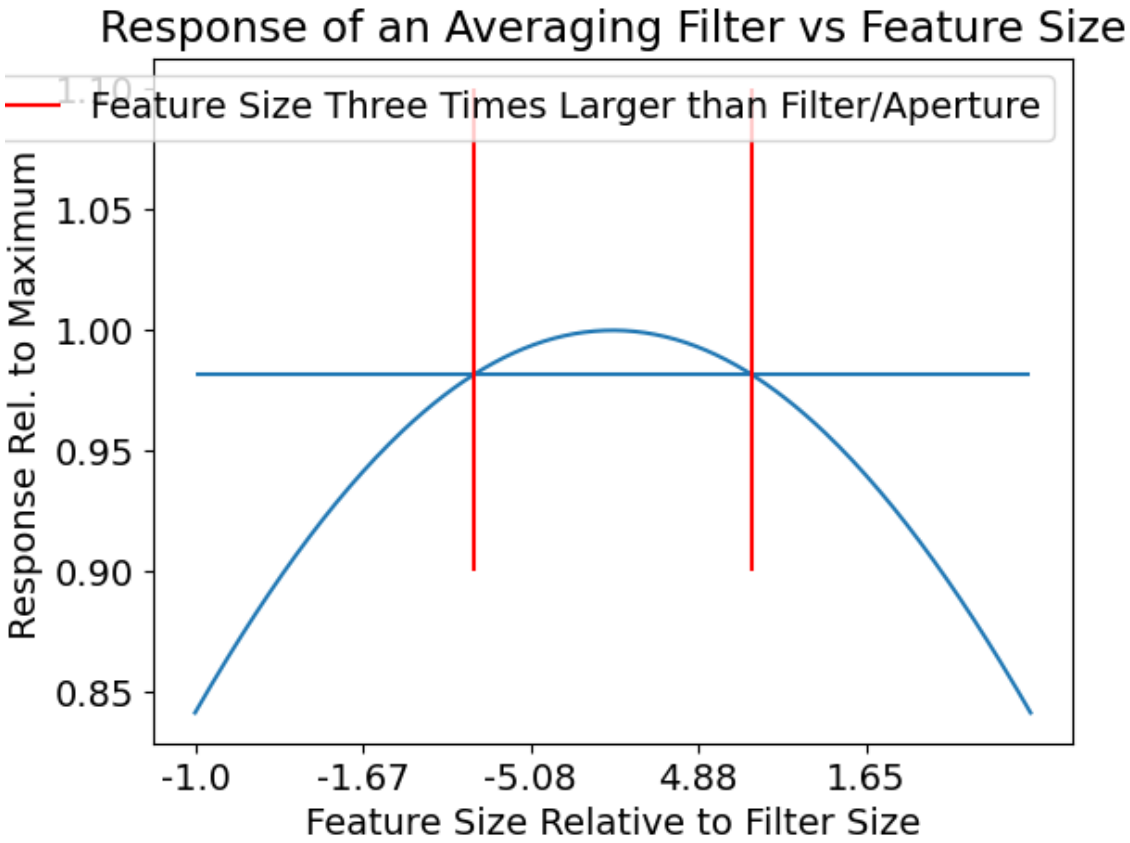

Figure 10: Gain factor relative to maximum for an averaging filter, ignoring constant complex phase, parameterized in terms of Fourier modes. The x axis is labled in terms of feature size. As expected smaller features are suppressed more heavily by an averaging, whereas features of infinite extent, equivalent to zero frequency(center of the plot) are completely unreduced. Taking values from this plot allows us to determine how much a digital filtering application to our derivative data would obscure/warp the features of the profile we are interested in.

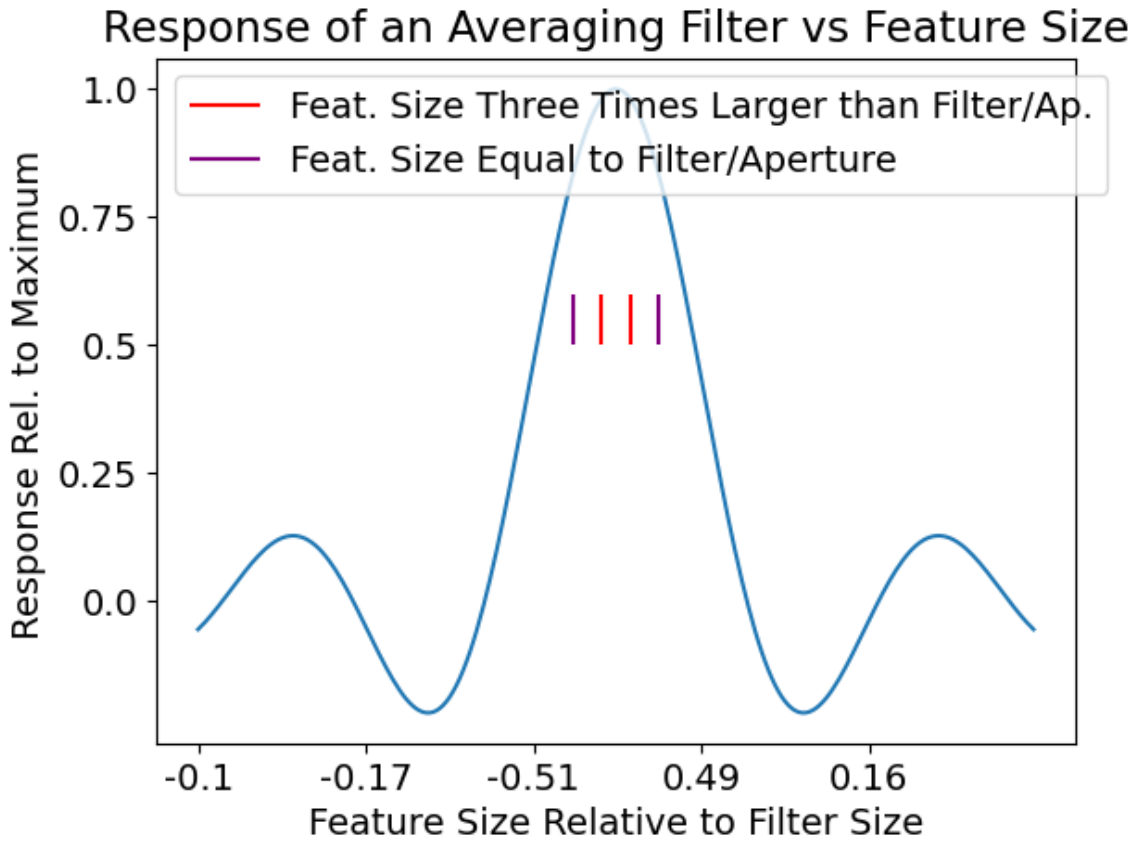

Figure 11: The same plot but zoomed out, revealing the filter response for even smaller features, which follows the sinc function (The Fourier transform of the rectangular impulse). It is now clear why we can filter out the induced increase in noise from the derivative easily. The feature size flickering electronic noise is mostly characterized by features of order 1-10 steps because of the low correlation between electronic noise through time. Since our filter is of order 1000 steps, the noise will be suppressed by about 100 times, whereas the slowly varying or large features of the signal will be mostly unchanged.

The finite derivative's feature size dependent gain function is also of the same family of curves as the averaging filter, which oscillate sinusoidally about $\omega = 0$, $e^{i\theta}G_{fin.der.}(\omega) = \frac{2}{\omega}(cos(\omega) - 1)$, but the peak in the gain factor is for feature sizes slightly larger than the derivative window(with next neighbor finite differentiation, this is two samples wide), and unsurprisingly $\omega = 0$ features are completely damped to zero amplitude by the finite derivative. Note that this gain function is approximately equal to the linear gain heuristic 8 given above, when ω is small. This makes sense, since in the limit of an infinitely small derivative filter, approaching the true derivative, the filter sees any continuous signal as slowly varying/of a large feature size. The important feature of this gain is that it amplifies high frequencies, which represent noise and details we cannot hope to measure, in our experiment. As a result unwanted noise is expected, and identified in experiment data after taking the finite derivative on our razor blade curves. An averaging filter carries an almost opposite behavior about its center, amplifying large features relative to small features, and can be used to counteract the increased noise of the finite derivative.

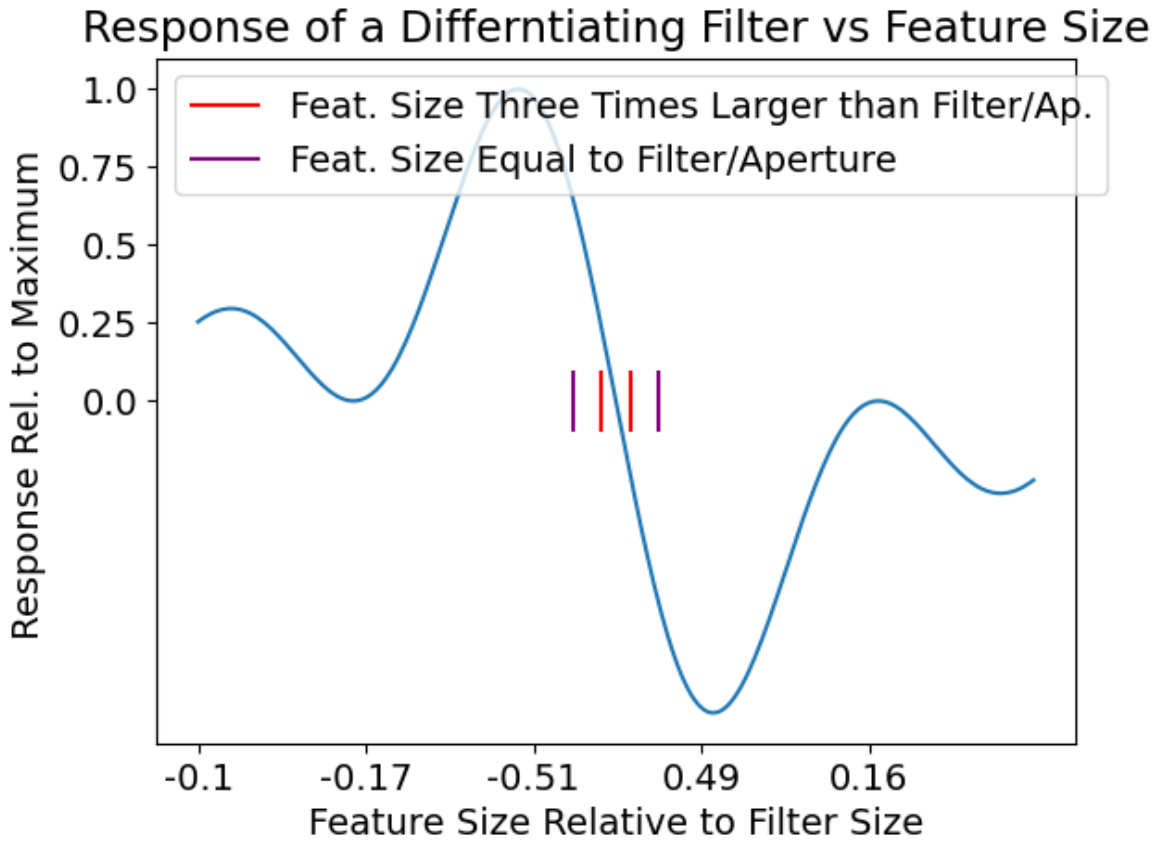

Figure 12: Filter response for a finite derivative up to a constant complex phase. Note the linear region for large features relative to the filter.

3.6. Results

Using the described methodology a collection of different slits were measured with one or both of the two profiling techniques. Errors are reported with high confidence interval notation (a,b) or with symmetric high confidence interval notation $\pm$. Because error was determined for the microscope and diffraction fitting completely due to a human's ability to measure distances with marked rigid geometries, and the measurer was not characterized statistically for their accuracy or precision, the meaning of high confidence as a probability is not perfectly defined, but can be taken to be relatively high, above 90%, since each measurement is based off of a small collection of measurements (Five or less) where a human measured a distance using a rigid marked measurement reference, and the chances of misreading such a device are very small for experienced users. In terms of curve fitting on the measured diffraction patterns, response of averaging filters, which can model the significantly finite aperture size of the pinhole, or the applied software filter for the razor method, explains most inconsistencies between model and data, namely flattened peaks, and missing finer modes, which are due to small feature suppression of such averaging/constant window filters. The contrast parameter seems to be set unreasonably high by model fitting, which results in troughs that are lower in the measured data than in the theory data, which is not what one would expect viewing an aperture as a linear average filter. Although it may be possible given that for some feature sizes, the rolling average filter has negative gain, which means it could cause these

higher order modes to become suppressors of the signal, despite their increase in the signal when the aperture/average window is infinitely small. This explanation could fail easily however, and there is a good chance experimental error is lurking, although cannot be investigated further due to time limitations.

Diffraction Profiling Slit Geometry Values Fit Parameters for Slit Width, Separation.

Aperture Width The apparent aperture width along the pattern was found to be $0.002m \pm 0.0001m$ for pinhole imaging.

Table 4

Method	Num. Slits	Slit Width, Error:(Upper, Lower)mm	Slit Separation (Upper, Lower)mm
Pinh.	1	0.079 (0.075, 0.083)	NA
Pinh.	2	0.043 (0.041, 0.045)	0.125 (0.120, 0.131)
Pinh.	3	0.044 (0.042, 0.046)	0.125 (0.119, 0.131)
Pinh.	4	0.043 (0.041, 0.045)	0.124 (0.119, 0.130)
Pinh.	5	0.043 (0.041, 0.045)	0.124 (0.118, 0.130)
Razor	1	0.090 (0.067, 0.112)	NA

Microscope Slit Geometry Values Microscope Measurements For Slit Width, Separation. Microscope was out of focus for measurement of underlined values, and thus these values may be inflated significantly above their true value. Each slit was not measured individually, instead one pair was measured in their separation and width, and used to characterize all other slits, since all slits were marked as being manufactured with the same separation and width, with the exception of the single slit which was measured separately.

Table 5

Num. Slits	Slit Width mm	Slit Separation mm
1	0.083 ± 0.004	NA
2	$\underline{0.051} \pm 0.004$	$\underline{0.130} \pm 0.004$
3	$\underline{0.051} \pm 0.004$	$\underline{0.130} \pm 0.004$
4	$\underline{0.051} \pm 0.004$	$\underline{0.130} \pm 0.004$
5	$\underline{0.051} \pm 0.004$	$\underline{0.130} \pm 0.004$

Manufacturer Slit Geometry Values Manufacturer did not provide error bars.

Table 6

Num. Slits	Slit Width mm	Slit Separation mm
1	0.08	NA
2	0.04	0.125
3	0.04	0.125
4	0.04	0.125
5	0.04	0.125

Airy Rings Observation With more precise equipment and the same techniques circular diffraction from small pinholes, also known as Airy Rings could be measured. During our experiment no data on these rings were produced, they were only observed to exist with the human eye. A circularly symmetric oscillating intensity pattern was seen on a target when laser light was shone perpendicularly on a hole of radius $400\mu m \pm 4\mu m$. The pattern qualitatively agreed with theory, as mentioned, the pattern was circularly symmetric, oscillating radially, and was most intense for low radii, going to no intensity for large radii or equivalently large angles to the center axis.

4. Discussion

Across all methods slit separations agreed between the microscope, diffraction, and manufacture measurements of the parameter. Even with possible parameter inflation due to a badly focused microscope. Slit widths did not agree as well between the microscope method, the manufacturer width and diffraction determined width. It is likely this failure of agreement is due to the aforementioned unfocused microscope, however if more experimentation time was permitted the diffraction method should also be further scrutinized, in addition to simply focusing the microscope better as to not inflate measured values.

5. Conclusion

Agreement was generally expected and observed, except the discussed microscope focusing failure, resulting in microscope slit widths falling outside the range estimated by diffraction measurement. These microscope measurements clearly must be repeated with a correctly focused image, as to not cause potential measurement error. The razorblade and pinhole method both created data that fit theoretical models of Fraunhofer diffraction. Because the measured slit widths, separations and manufacturer slit widths, separations matched well, it is concluded that the theoretical model is likely valid for these laboratory conditions. Further investigation is clearly needed especially to remeasure slit widths with the microscope, as the slit width values obtained that are likely inflated fail to agree, and cast significant doubt on the validity of the theoretical model if they are accurate slit width values. This can only be determined with further measurement, and so the theory should be tentatively accepted, given the small range of disagreement, and the expected inflation of parameters (microscope measured slit width) likely causing such disagreement. Any investigation using such theory without further measurement/independent confirmation of Fraunhofer diffraction would not be well founded.

Comparing the two diffraction methods, razorblade diffraction is much faster, and more flexible in that it effectively has software adjustable aperture size, given the blocking target moves so little compared to the feature sizes of the diffraction patterns, which means its effective physical aperture is very small. Razorblade method is recommended as the method of choice if only razorblade and pinhole methods are viable. Measurement by camera can be much faster than either, requiring a single image to capture the central portion of the diffraction pattern, but requires different equipment.

The same model fitting, but with the special function that describes Airy circular diffraction in terms of its radial coordinate on the target/observing plane, since the pattern is circularly symmetric, would be viable to convert data from these rings into parameters such as aperture radius. A radial coordinate could be established by either physically aligning a scan along an axis of the Airy pattern, or imaging the entire pattern with a camera sensor, then finding the ”center of mass” of this 2d

image, to define distances that are the radius/radial coordinate. The distance from the 2d "center of mass" coordinate can be defined as the radius, and an average can be taken over all the different angles for each constant radial coordinate to use all available data. Of course taking an average over angle at different radii needs to be done carefully, since the area of a circular disc segment is a function of r: $dA = 2\pi r dr$. When averaging intensities at a radius, this formula needs to be used, or discrete pixel counting, to ensure the average is done correctly.

The radial portion of the Airy diffraction pattern is a Bessel function of the radial displacement on the target. For curve fitting purposes this Bessel function highly resembles the sinc function, and thus fitting the radial variation of the Airy pattern could be done with contrast and phi factors aswell to allow for better fit convergence. Then one could analyze the output parameter covariance matrix, and perturbations on the fixed parameters to find out wether fixed parameters, fit parameters, or both were large contributors to error, and do error analysis from there if necessary to combine these errors.